Langmuir

Article

pubs.acs.org/Langmuir

Direct Electroplated Metallization on Indium Tin Oxide Plastic Substrate

Nga Yu Hau,[†,§] Ya-Huei Chang,[†,§] Yu-Ting Huang,[†] Tzu-Chien Wei,[‡] and Shien-Ping Feng*[,†]

[†]Department of Mechanical Engineering, The University of Hong Kong, Pokfulam, Hong Kong

[‡]Department of Chemical Engineering, National Tsing-Hua University, Hsinchu, Taiwan

Supporting Information

ABSTRACT: Looking foward to the future where the device becomes flexible and rollable, indium tin oxide (ITO) fabricated on the plastic substrate becomes indispensable. Metallization on the ITO plastic substrate is an essential and required process. Electroplating is a cost-effective and high-throughput metallization process; however, the poor surface coverage and interfacial adhesion between electroplated metal and ITO plastic substrate limits its applications. This paper develops a new method to directly electroplate metals having strong adhesion and uniform deposition on an ITO plastic substrate by using a combination of 3-mercaptopropyl-trimethoxysilane (MPS) self-assembled monolayers (SAMs) and a sweeping potential technique. An impedance capacitive analysis supports the proposed bridging link model for MPS SAMs at the interface between the ITO and the electrolyte.

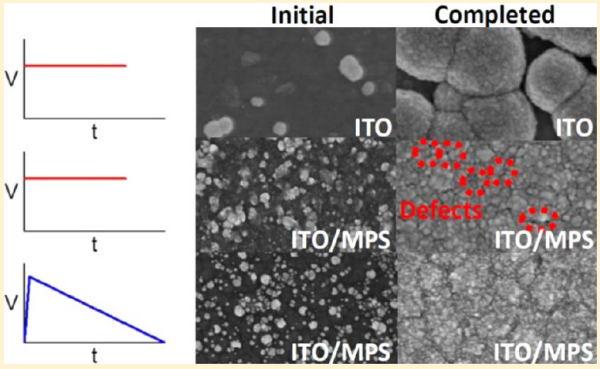

1. INTRODUCTION

Indium tin oxide (ITO) having superior optical and electrical properties has been widely fabricated on glass as a substrate in optoelectronic applications, such as thin-film transistors, flat panel displays, light-emitting diodes (LED), optical sensors, electrochromic windows, and photovoltaic cells. Thermal evaporation, pulsed-laser deposition and sputtering techniques are the most common methods to fabricate transparent conducting ITO thin films (150−200 nm) on glass substrates at a temperature of 300−350 °C.[1,2] Metallization on ITO substrate is crucial to various purposes in devices, such as silver interconnects for device-to-device integration, gold current collectors in optical sensors, and platinum counter electrodes in dye-sensitized solar cells.[3−6] It is relatively common to screen-print a metal over ITO surface with a conductive paste. After burning out polymer binders by postannealing at a temperature of 200−500 °C, a conductive metal layer can be formed on the ITO surface. Toward the future where the device goes flexible and rollable, ITO fabricated on a plastic substrate becomes indispensable. Contrary to the rigid glass, the polymeric substrates, such as polyethylene naphthalate (PEN) or poly(ethylene terephthalate)(PET), cannot withstand the high temperature so that ITO has to be coated by using rf or dc magnetron sputtering at low temperature (<100 °C).[2] Thus, the ITO-PEN generally has a relatively high sheet resistance (15−30 Ω/□) and poor wettability. To achieve metallization on ITO-PEN, a low-temperature conductive paste was invented to avoid the high temperature in the postannealing, but it performs relatively high resistance due to the unavoidable impurities remaining in the finished metal layer.[7,8] Sputtering is another method to fabricate a metal layer on the ITO-PEN. However, it is time-consuming and requires costly vacuum equipment. In addition, the relatively poor wettability of the ITO surface causes the sputtered metal atoms to more preferably bind to each other than to the ITO surface and grow into islands so that it needs an additional thin layer, such as sputtered chromium or titanium between the metal and substrate, to improve adhesion.[9]

Electroplating is another very commonly used metallization process for electronic components, printed circuit boards, and semiconductor industries in the past century due to its inherently low cost, low temperature, and high throughput. Metals employed for such purposes include copper, nickel, tin, cobalt, chromium, silver, gold, and their respective alloys. However, compared with the metal surface, the ITO surface has a relatively low surface energy and high sheet resistance, leading to high nucleation energy for electroplating. As a consequence, scattered, and irregular grain growth on a small number of nucleation sites causes poor surface coverage.[10] Furthermore, strain and stress, originating from the different atomic arrangement of the two adjacent layers, increase with increasing film thickness, leading to a poor interface adhesion.[11,12] In brief, the ITO surface does not provide opportunities to strongly interlock the electroplated metals and the substrates.

This paper therefore aims to directly electroplate metals having strong adhesion and uniform deposition on ITO-PEN.

Received: August 14, 2013
Revised: December 23, 2013
Published: December 23, 2013

   dx.doi.org/10.1021/la404552c | *Langmuir* 2014, 30, 132−139

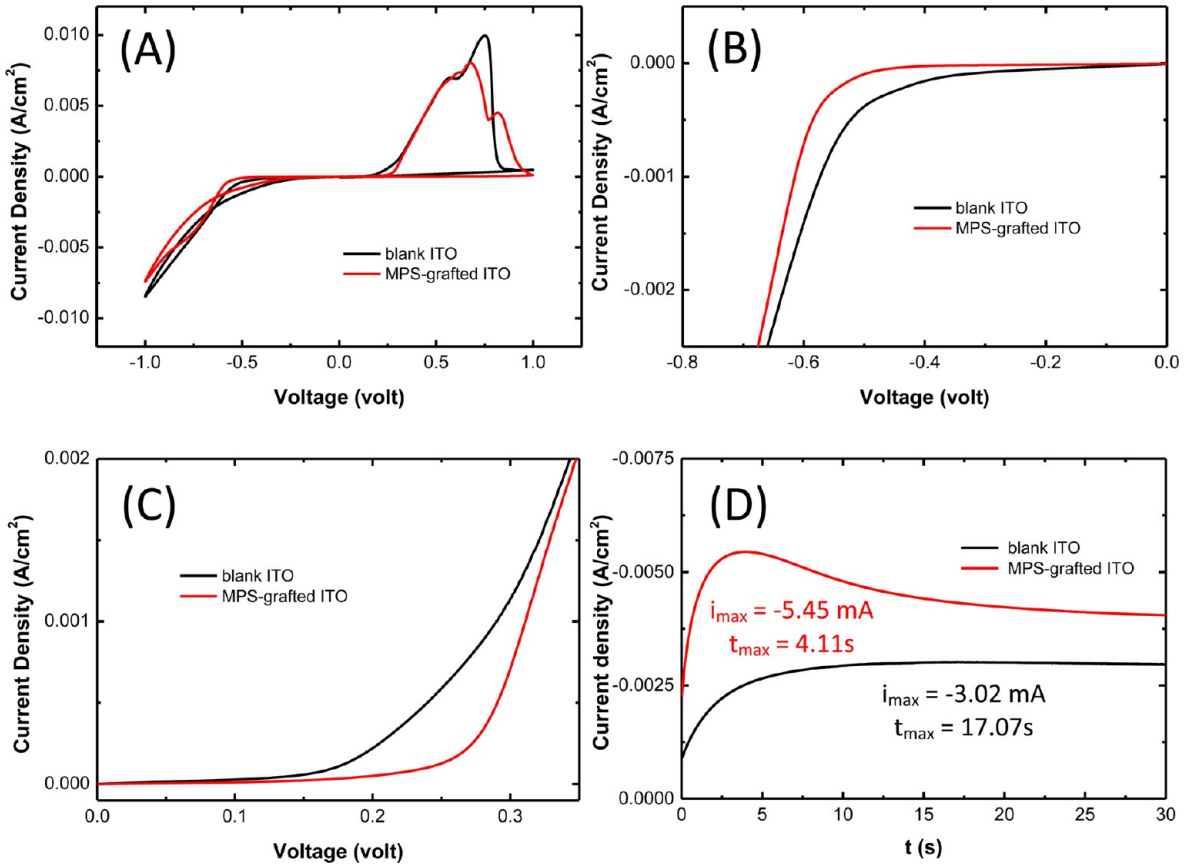

Figure 1. (A) Cyclic voltammetry for silver on ITO PEN with and without MPS pretreatment. (B) Cathodic waves of cyclic voltammetry. (C) Anodic waves of cyclic voltammetry. (D) Chronoamperograms of electroplating silver under operating voltage of −0.8 V on blank and MPS-grafted ITO plastic substrates.

We present a new technique to overcome the difficulties of the initial nucleation process for electroplating metals on ITO-PEN by using a combination of 3-mercaptopropyl-trimethoxysilane (MPS) self-assembled monolayers (SAMs) and sweeping potential electrodeposition. This finding is expected to provide a low temperature, cost-effective, and reliable metallization on ITO-coated plastic substrates to facilitate the electronic devices to be flexible, rollable, and lightweight in the future.

2. EXPERIMENTAL SECTION

ITO-PEN (1.5 cm × 2 cm) having a sheet resistance of 15 Ω/□ and optical transmission of 75% was cleaned by immersion into a 4% PK-LCG545 (Parker Corp.) and DI water bath at 50 °C for 15 min with sonication, respectively. For MPS pretreated samples, the substrates were immersed into a solution of 1% MPS in ethanol for 30 min at room temperature. Contact angle was measured by a static contact angle goniometer (Sindatek model 100SB). A chemical-resist sticker (Max Bepop, CM-200E) was used as a mask with an interior 1 cm^2 hollow circle to predetermine the electroplated area on the substrate. The experiments were then carried out by silver electroplating on blank and MPS-pretreated ITO-PEN under constant potential or sweeping potential methods from a commercial silver electrolyte (Metaler MetSil 500CNF R-T-U; contents, 0.28 M of silver ions, cyanide free) at room temperature. Electrochemical measurements, including chronoamperometry, chronocoulometry, cyclic voltammogram, and electrochemical impedance spectroscopy were performed using a CHI 660E workstation. Platinum mesh and silver/silver chloride (Ag/AgCl) were used as the counter electrode and the reference electrode, respectively, in a standard three-electrode system. The interface contact performance between silver and ITO-PEN was evaluated by the change of electrical resistance versus bending cycles. For the bending test, one end of the sample was fastened while the other was free to move vertically over a certain distance by rotation of the crank. (The bending test device and its corresponding angular rotation are shown schematically in Figure 6A.) Then, the two-point probe dc method with a fixed distance of 1 cm (one end on the silver coating and the other end on the ITO-PEN) was used to measure electrical resistance by a multimeter.

3. RESULTS AND DISCUSSION

As known, the initial stage of electroplating on low surface energy substrates, such as ITO-PEN, corresponds to the instantaneous nucleation model where the growth of nuclei on a small number of active sites (relative high surface energy) occurs in a very short time period.[10,13−15] Then, these nucleation sites grow into islands and coalesce. Island growth mode is usually not preferable for technological applications due to its poor adhesion and nonuniform deposition. In the case of electroplating, if the film wets poorly, the atoms preferably bind to each other than to the substrate, causing the island growth. Conversely, good wetting makes the atoms more strongly bind to the substrate than to each other. Therefore, one approach to improve electroplating nucleation is to yield a wettable surface that facilitates the subsequent metallization. The other method is to use a bridging ligand, such as sulfide, to link metal ions as a promotion agent during electroplating.[16−18] Functionalized self-assembled silane monolayers (SAMs) have been used for many years as corrosion prevention for various substrates and adhesion promoter for jointing two substrates (metal sheets, polymer films) by chemical or electrostatic

dx.doi.org/10.1021/la404552c | Langmuir 2014, 30, 132−139

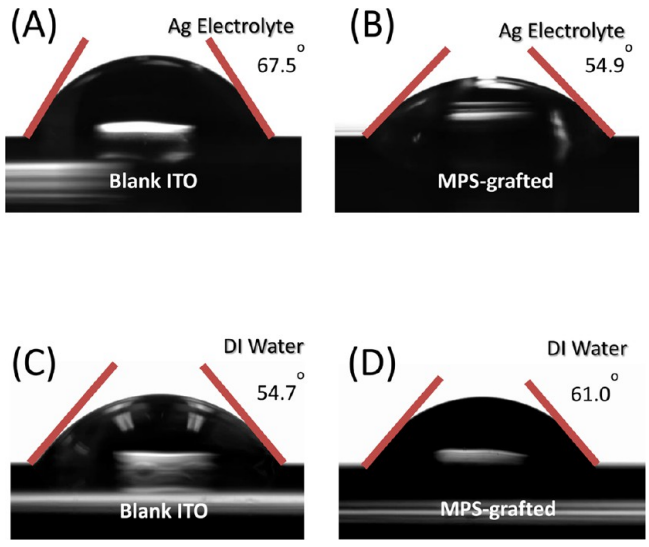

Figure 2. Contact angles of silver electrolyte on (A) blank and (B) MPS-grafted ITO-PEN. Contact angles of water on (C) blank and (D) MPS-grafted ITO-PEN.

binding.[19] Recently, it was discovered that some SAMs are able to transport electrons by the hopping process to enhance electrochemical or photochemical reactions.[20,21] The 3-mercaptopropyl-trimethoxysilane (MPS) with the hydrolyzable methoxy end-group would adhere to the ITO surface, and its sulfur functional group can perform the role of a bridging-link to metal ions in the electrolyte. According to the concepts mentioned above, MPS is therefore chosen to promote nucleation and adhesion for electroplating metal on ITO-PEN.

Figure 1A shows a current−potential curve from cyclic voltammetry (CV) for silver on ITO-PEN with and without MPS pretreatment. Figure 1B,C are the corresponding cathodic wave and anodic wave of Figure 1A, respectively. Compared with blank ITO surface, silver electrodeposition on MPS-pretreated surface occurs at a more negative onset voltage because an additional energy is required for electron hopping across nanometer-thick MPS monolayers to reduce silver ions, as shown in Figure 1B. Figure 1C shows a more positive onset voltage in an anodic wave for MPS-pretreated surface, indicating that the deposited silver atoms bond more strongly on ITO-PEN so that the oxidation process is relatively hard to occur. In general, a conductive substrate in redox-active electrolyte can be expressed as the electrolyte resistance in series with a generic scheme involving a faradaic charge transfer

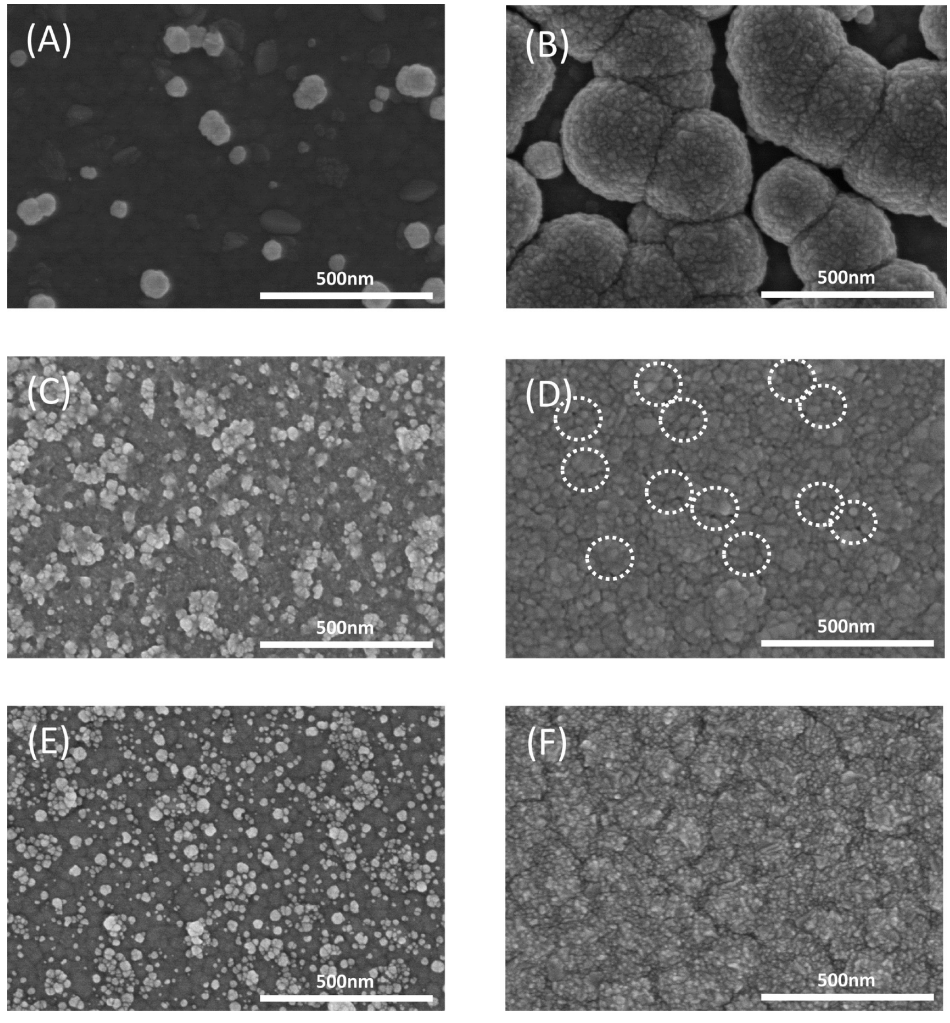

Figure 3. SEM images of electroplated silver on blank and MPS-pretreated samples at initial (0.0016 C) and completed electroplating stages (0.088 C).

dx.doi.org/10.1021/la404552c | *Langmuir* 2014, 30, 132−139

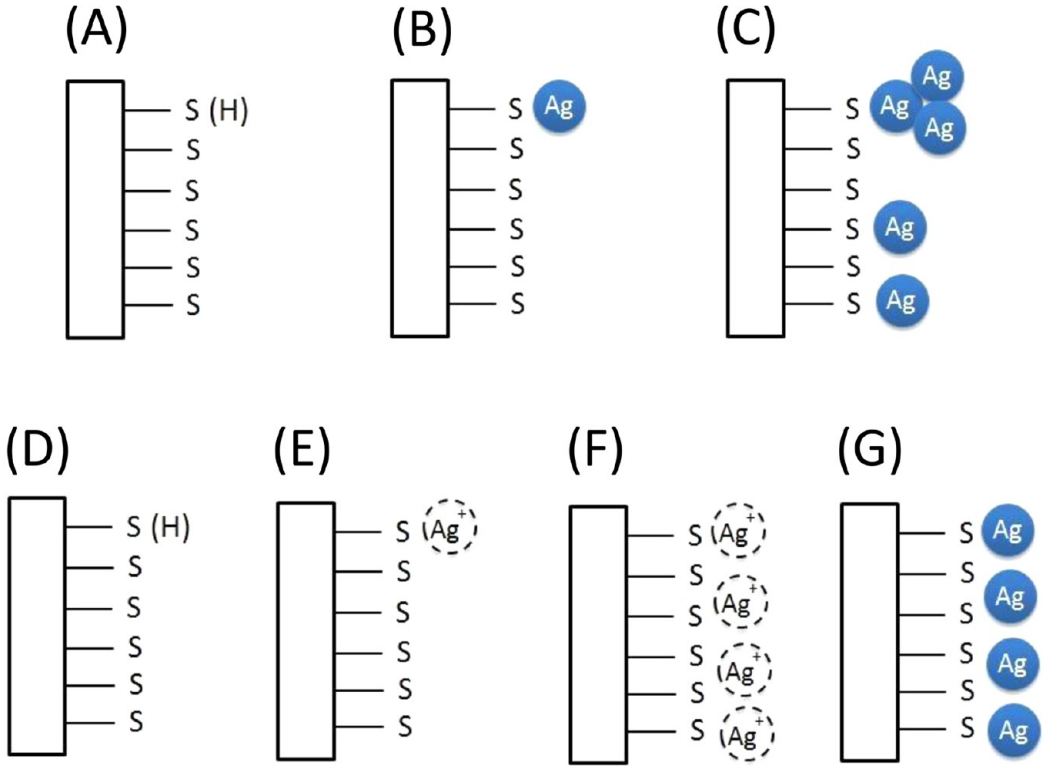

Figure 4. Schematic diagram for silver eletrodeposition using constant potential on (A) MPS-grafted ITO-PEN surface, (B) silver ions nucleate on the high surface energy sites *S*(*H*), (C) silver ions nucleate on the other active sites and also deposit on formed nuclei. The schematic diagram for silver electrodeposition using sweeping-potential on (D) MPS-grafted ITO-PEN surface, (E) silver ions occupy the high surface energy sites *S*(*H*), (F) silver ions link to other available active sites by increasing potential, (G) silver ions are reduced to atoms when potential increases over the onset voltage.

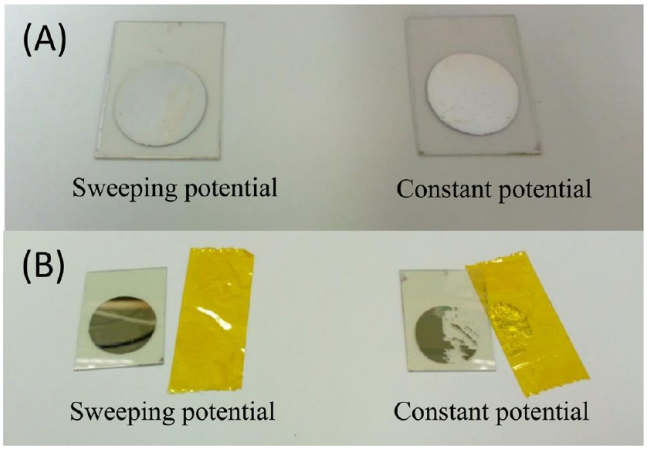

Figure 5. (A) Electroplated silver at constant potential and sweeping potential on MPS- pretreated ITO plastic substrate. (B) Pull-off adhesion test performed using 3 M flatback Masking tape 250 (ASTM D3359).

resistance (R_{ct}) parallel to a nonfaradaic electrochemical double-layer capacitance (C_{dl}). The chronoamperograms in Figure 1D are the current responses at an operating voltage of −0.8 V for electroplating silver on ITO-PEN without and with MPS treatment. According to the Scharifker-Hills model, the nuclei population density is inversely proportional to the square of the peak current (i_{max}) multiplying by the corresponding peak time (t_{max}) in the chronoamperograms. Electroplating silver on blank and MPS-grafted ITO-PEN is correlated to the instantaneous nucleation mode. The calculated silver nuclei densities on blank and MPS-grafted ITO-PEN are 2.69×10^6 and 4.4×10^{10} cm^{-2}, respectively (see the Supporting Information, section 1). The significant increase of nuclei density provides evidence that the presence of MPS monolayers perform like a bridge to link the silver ions in electrolyte, which is thereby beneficial to the subsequent electrodeposition. It was reported that the presence of SAMs and adsorbed ions introduces a field-induced dipole that profoundly increases the adsorbed charges and shortens the distance of the electrochemical double layer.[22−24] Thus, when electroplating, the nucleation process can be readily generated by electron hopping which can reduce the linked silver ions to atoms. Figure 2A,B shows that the contact angle of silver electrolyte on MPS-grafted ITO-PEN is smaller than that on the blank surface. Figure 2C,D shows an opposed trend when using DI water as a liquid probe. The wettability is only improved in the case of using silver electrolyte, resulting from the bridging-link effect between silver ions and the MPS monolayers.

Figures 3A−F are field-emission scanning electron microscopy (FE-SEM) images of electroplated silver on blank and MPS-pretreated samples under constant potential and sweeping potential eletrodeposition at initial (parts A, C, and E with the plating charge of 0.0016 C) and completed electroplating stages (parts B, D, F with the plating charge of 0.088 C). As seen in Figure 3A, the uneven and randomly distributed silver nuclei are initially electrodeposited on a few active sites of blank ITO-PEN. The following silver ions are preferentially reduced on the small number of silver nuclei in order to minimize surface energy and then coalesce, leading to a large irregular grain structure with poor surface coverage in Figure 3B. Figure 3C,D

dx.doi.org/10.1021/la404552c | *Langmuir* 2014, 30, 132−139

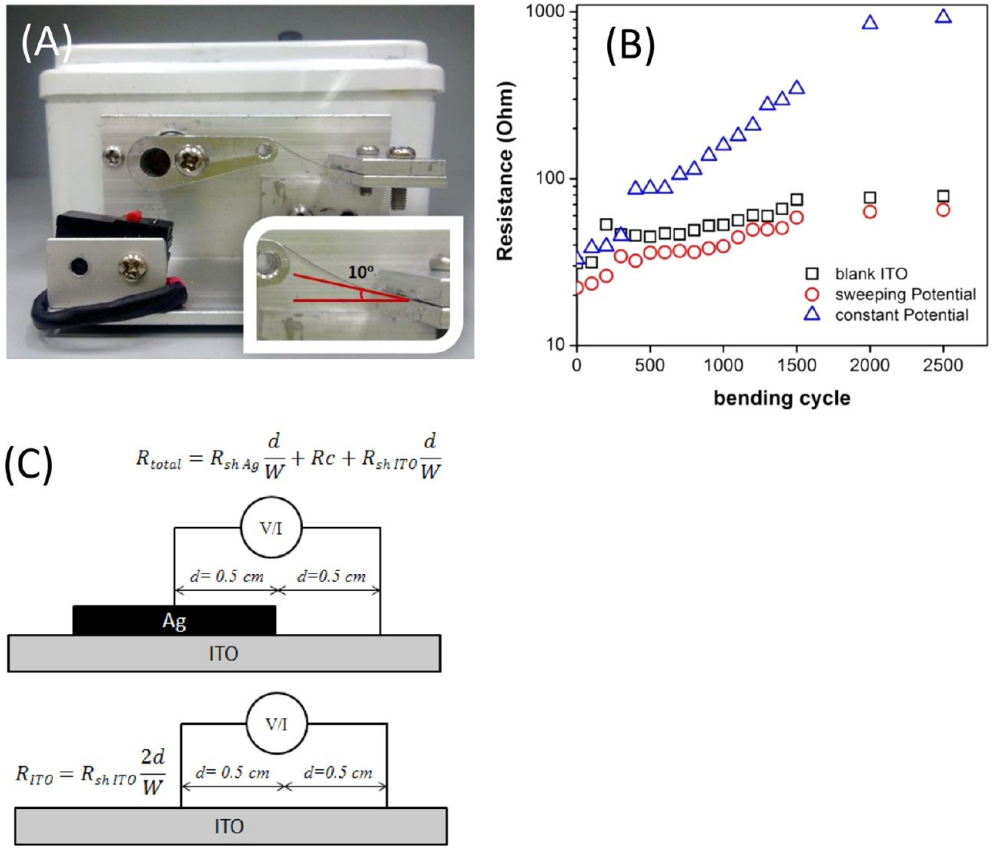

Figure 6. (A) The bending test device with the corresponding angular rotation. (B) The change of electrical resistance versus bending cycles for blank ITO-PEN and electroplated silver on MPS-grafted ITO-PEN using the constant-potential and sweeping-potential methods. (C) Schematic diagram of two-point probe dc method for resistance measurement (R_{total} is the total measured resistance, R_{sh} is the sheet resistance, R_c is the contact resistance, W is the width of silver coating, d is the measured spacing).

show that the presence of MPS monolayers effectively promotes the formation of nucleation sites to achieve a full coverage of silver deposit with a thickness of 160 nm (measured by KLA-Tencor P16 profilometer). However, there are some pits and voids found in the silver deposit as circled in Figure 3D, which could be attributed to the agglomerated nucleation clusters (as seen in Figure 3C) causing localized uneven distribution in sizes of nuclei, therefore, leading to localized uneven grain growth. In general, full coverage of SAMs can be quickly obtained from millimolar solutions, but the density and defects are varied substantially dependent on the morphology of polycrystalline ITO film on plastic substrates, such as crystal defects, atomic step, grain edge, and impurities. Therefore, the resulting MPS monolayers have a range of distribution in densities and defects, reflecting a distribution of surface energy. Given a constant operating potential, silver ions will be reduced to atoms on the high surface energy sites on MPS monolayers as the first nuclei. Then, silver ions nucleate on the other active sites and also deposit on formed nuclei. Therefore, before entering the next stage for bulk grain growth, the first nuclei have grown into clusters resulting in the uneven distribution in sizes of nuclei. To improve this, the potential sweeping forward at 0.5 V/s from 0 to −1 V and then reversed at 0.02 V/s from −1 to 0 V is introduced to compensate the surface energy distribution of MPS monolayers. When the potential is swept at a low voltage, the silver ions in the electrolyte preferentially occupy the high surface energy sites on MPS monolayers. Subsequently, the increase of potential only keeps forcing the silver ions linking to other available active sites on the MPS layer because no reduction reaction occurs before the onset voltage. Once the potential exceeds the onset voltage, electrons hop across the MPS monolayers to reduce all the linked silver ions to atoms, evenly generating more nucleation sites without agglomerated clusters, as seen in Figure 3E. A conformable silver electroplated coating with a fine grain size can be achieved, as shown in Figure 3F. The schematic diagram is shown in Figure 4 for electroplating silver on MPS-grafted ITO-PEN using constant potential and sweeping potential methods.

Referring to Figure 5, the pull-off adhesion test using 3 M flatback masking tape 250 (ASTM D3359) shows that almost all of the coating was stripped off for electroplated silver on MPS-grafted ITO-PEN at constant potential. As mentioned above, the agglomerated nucleation clusters result in localized uneven grain growth, which increases stacking fault, film stress, and strain due to a mismatch in the lattice spacing. Therefore, the poor adhesion can be understood as a weak interface contact between the electroplated film and the substrate. In contrast, no coating came off for electroplated silver using the sweeping potential technique on the MPS-grafted sample. It is believed that the deposited atoms which grow on the uniformly nucleated layer could achieve the improved adhesion. Apart from a good mechanical contact performance, fabricating a reliable electrical contact between metal and ITO-PEN is of prime importance in optoelectronic applications.

Figure 6B shows the change of electrical resistance versus bending cycles measured by a two-point probe method for blank ITO-PEN and 160 nm electroplated silver coating on

dx.doi.org/10.1021/la404552c | Langmuir 2014, 30, 132−139

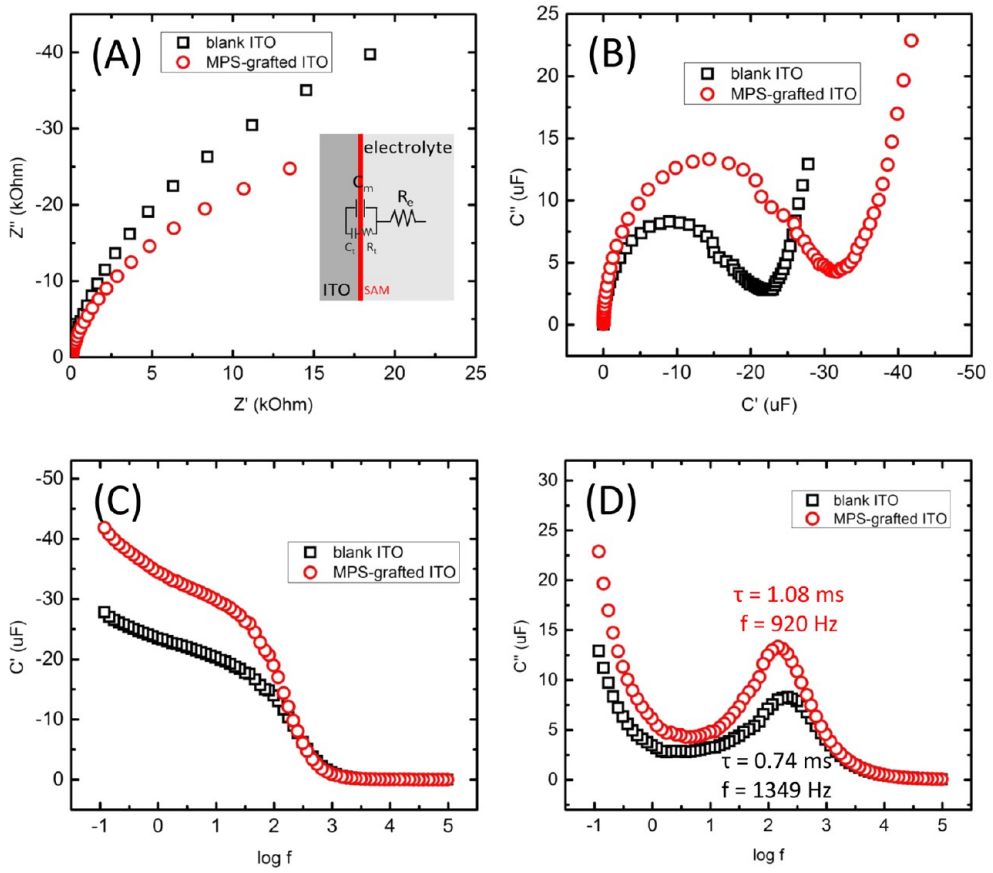

Figure 7. Electrochemical impedance spectroscopy (EIS) characterization for blank ITO-PEN and MPS-grafted ITO-PEN in a supporting electrolyte of 0.2 M KNO_3: (A) Nyquist plots, (B) Corresponding Nyquist capacitive plots. Bode plots of the (C) real and (D) imaginary parts of the complex capacitance.

MPS-grafted ITO-PEN by using constant potential and sweeping potential methods. The measured resistance (R_{total}) between the two points includes the resistance of silver layer ($R_{sh\ Ag} \sim 2\ \Omega/Y$), the resistance of ITO-PEN ($R_{sh\ ITO} \sim 15\ \Omega/Y$), and their contact resistance (R_c), as shown in Figure 6C. As noted in the equations, if R_c is low and negligible, the total measured resistance of Ag-coated sample is normally lower than that of blank ITO-PEN. The samples using constant potential and sweeping potential methods exhibit the behavior of ohmic contact between silver coating and substrate (see the Supporting Information, Section 2). For blank ITO-PEN, the resistance increases versus bending cycles because the mechanical bending usually causes tiny cracks in the conductive ITO layer. For the constant potential sample, the total resistance dramatically increases with the increasing number of bending cycles, which can be explained by its poor interfacial adhesion resulting in the increase of contact resistance so that it hinders electron transfer from the silver coating to the ITO substrate. For sweeping potential samples, the increase of resistance follows the same trend as blank ITO after 2500 bending cycles, demonstrating a reliable contact between the electroplated silver and ITO-PEN. This finding also proves that the presence of the MPS monolayers at the interface does not hinder the electron transfer.

To further investigate the ITO/MPS/liquid interface, electrochemical impedance spectroscopy (EIS) is used to characterize the interfacial behaviors in a supporting electrolyte of 0.2 M KNO_3. This is a nonredox-active solid/SAM/liquid junction where only nonfaradaic processes are involved so that the capacitive characteristics are pronounced rather than the resistive terms. Figure 7A,B summarizes the Nyquist impedance and capacitance spectroscopy, showing that MPS-grafted ITO enhances the capacitive characteristics compared with blank ITO. As mentioned, the SAM molecular layer would induce an ion-dipole capacitance by linking to associated ions in the electrolyte.[23−25] Therefore, the increase of capacitance can be explained by the bridging link effect between the sulfur functional groups of MPS and the silver ions in the electrolyte, which is consistent with the above-mentioned results in Figure 1B. Equivalent circuit model of the ITO/liquid interface is the contribution from an electrolyte resistance (R_e) in series with a double-layer capacitor (C_{dl}). In the case of the ITO/MPS/liquid, the equivalent circuit model can be expressed as the electrolyte resistance in series with a generic scheme which encompasses a series capacitor (C_t) and a resistance (R_t) parallel to a high-frequency capacitor (C_m). As known, the perturbation of C_{dl} generates an equivalent capacitance term C_m at high frequency. The response of the ionic dipolar MPS terms is represented by the series resistive (R_t) and capacitive terms (C_t), which are coupled and the associated relaxation time $\tau = R_tC_t$.[25] The Bode plot of the real part of the complex capacitance provides a facile means of quantifying the C_t contribution, corresponding to the plateau at low frequency in Figure 7C. The Bode plot of the imaginary part of the complex capacitive function directly reports the angular characteristic frequency of the relaxation resonance $\tau = \omega^{-1}$, as shown in Figure 7D. In accordance with the previously noted mechanism, there is a bridging-link interaction between MPS-

dx.doi.org/10.1021/la404552c | Langmuir 2014, 30, 132−139

grafted ITO and electrolyte ions so that the relaxation time τ retards due to the enhancement of capacitive behavior. To advance our understanding, we further investigated the capacitance spectroscopy for MPS, APTS ((3-aminopropyl)-triethoxysilane) and TPS (trimethoxy(propyl)silane) grafted on ITO-PEN, which supports the above-mentioned mechanism that MPS serves as an effective bridging-link layer to promote the electroplated metallization (see the Supporting Information, Section 3).

4. CONCLUSIONS

In this paper, a low-temperature and cost-effective method was developed to enable direct electroplated metallization on ITO-PEN by using a combination of MPS SAMs and sweeping potential electrodeposition. The MPS SAMs on the substrate provides the bridging-link between the sulfur functional groups and the silver ions in the electrolyte, facilitating the electroplating nucleation process. Compared with constant potential electroplating, more and even nucleation sites can be generated using sweeping potential electrodeposition on MPS-grafted ITO-PEN to achieve an improved adhesion. EIS measurement is used to analyze the interfacial capacitive characteristics of the MPS monolayers, which supports the bridging-link model. Pull-off tape test and resistance measurement versus bending cycles demonstrate that a reliable and low ohmic contact between electroplated silver and ITO-PEN can be achieved. This solution-based process would be applicable in the manufacturing of various metals on ITO-PEN beneficial for the devices to be flexible and rollable.

■ ASSOCIATED CONTENT

Supporting Information

Instantaneous and progressive nucleation models, ohmic contact between the ITO/MPS/silver interface, and measurement of EIS for different kinds of silane and EDS analysis. This material is available free of charge via the Internet at http://pubs.acs.org.

■ AUTHOR INFORMATION

Corresponding Author

*E-mail: hpfeng@hku.hk.

Author Contributions

[§]N.Y.H. and Y.-H.C. contributed equally to this work.

Notes

The authors declare no competing financial interest.

■ ACKNOWLEDGMENTS

This work was supported by the General Research Fund from Research Grants Council of Hong Kong Special Administrative Region, China, under Award Number HKU 719512E.

■ REFERENCES

(1) Lin, H.; Yuy, J.; Wang, N.; Lou, S.; Jiang, Y. Fabrication and Properties of DC Magnetron Sputtered Indium Tin Oxide on Flexible Plastic Substrate. *J. Mater. Sci. Technol.* **2009**, *25*, 119−122.

(2) Meng, Z.; Peng, H.; Wu, C.; Qiu, C.; Li, K. K.; Wong, M.; Kwok, H. S. Room-Temperature Deposition of Thin-Film Indium Tin Oxide on Micro-Fabricated Color Filters and its Application to Flat-Panel Displays. *J. Soc. Inf. Disp.* **2004**, *12*, 113−118.

(3) Chen, L. Y.; Chen, H. I.; Huang, C. C.; Huang, Y. W.; Tsai, T. H.; Liu, Y. C.; Chen, T. Y.; Cheng, S. Y.; Liu, W. C. Characteristics of an Electroless Plated-Gate Transistor. *Appl. Phys. Lett.* **2009**, *95*, 052105−052107.

(4) Chiang, K. K.; Chen, J. S.; Wu, J. J. Aluminum Electrode Modulated Bipolar Resistive Switching of Al/Fuel-Assisted NiO_x/ITO Memory Devices Modeled with a Dual-Oxygen-Reservoir Structure. *ACS Appl. Mater. Interfaces* **2012**, *4*, 4237−4245.

(5) Grätzel, M. Photoelectrochemical Cells. *Nature* **2001**, *414*, 338−344.

(6) Gong, Y.; Li, C.; Huang, X.; Luo, Y.; Li, D.; Meng, Q.; Iversen, B. B. A Simple Method for Manufacturing Pt Counter Electrodes on Conductive Plastic Substrates for Dye-Sensitized Solar Cells. *ACS Appl. Mater. Interfaces* **2013**, *5*, 795−800.

(7) Zhang, Z.; Lu, G. Q. Pressure-Assisted Low-Temperature Sintering of Silver Paste as an Alternative Die-Attach Solution to Solder Reflow. *IEEE Trans. Electron. Packag. Manuf.* **2002**, *25*, 279−283.

(8) Wang, T.; Chen, X.; Lu, G. Q.; Lei, G. Y. Low-Temperature Sintering with Nano-Silver Paste in Die-Attached Interconnection. *J. Electron. Mater.* **2007**, *36*, 1333−1340.

(9) Ikegami, M.; Miyoshi, K.; Miyasaka, T.; Teshima, K.; Wei, T. C.; Wan, C. C.; Wang, Y. Y. Platinum/Titanium Bilayer Deposited on Polymer Film as Efficient Counter Electrodes for Plastic Dye-Sensitized Solar Cells. *Appl. Phys. Lett.* **2007**, *90*, 153122−153124.

(10) Budevski, E.; Staikov, G.; Lorenz, W. J. Electrocrystallization: Nucleation and Growth Phenomena. *Electrochim. Acta* **2000**, *45*, 2559−2574.

(11) Feng, H. P.; Paudel, T.; Yu, B.; Chen, S.; Ren, Z. F.; Chen, G. Nanoparticle-Enabled Selective Electrodeposition. *Adv. Mater.* **2011**, *23*, 2454−2459.

(12) Feng, S. P.; Chang, Y. H.; Yang, J.; Poudel, B.; Yu, B.; Ren, Z. f.; Chen, G. Reliable Contact Fabrication on Nanostructured Bi_2Te_3-based Thermoelectric Materials. *Phys. Chem. Chem. Phys.* **2013**, *15*, 6757−6762.

(13) Lin, Z. B.; Xie, B. G.; Chen, J. S.; Sun, J. J.; Chen, G. N. Nucleation Mechanism of Silver During Electrodeposition on a Glassy Carbon Electrode from a Cyanide-Free Bath with 2-Hydroxypyridine as a Complexing Agent. *J. Electroanal. Chem.* **2009**, *633*, 207−211.

(14) Palomar-Pardavé, M.; Ramírez, M. T.; González, I.; Serruya, A.; Scharifker, B. R. Silver Electrocrystallization on Vitreous Carbon from Ammonium Hydroxide Solutions. *J. Electrochem. Soc.* **1996**, *143*, 1551−1558.

(15) Khelladi, M. R.; Mentar, L.; Azizi, A.; Sahari, A.; Kahoul, A. Electrochemical Nucleation and Growth of Copper Deposition onto FTO and n-Si (100) Electrodes. *Mater. Chem. Phys.* **2009**, *115*, 385−390.

(16) Chou, C. S.; Tu, H. C.; Wang, Y. Y.; Wan, C. C. Method to Accelerate Pd/Sn Based Direct Plating Process. *Electrochem. Solid-State Lett.* **2004**, *7*, C111−C114.

(17) Yang, C. H.; Wang, Y. Y.; Wan, C. C.; Chen, C. J. A Search for the Mechanism of Direct Copper Plating via Bridging Ligands. *J. Electrochem. Soc.* **1996**, *143*, 3521−3525.

(18) Yang, C. H.; Wang, Y. Y.; Wan, C. C. A Kinetic Study of Direct Copper Plating via Pd Catalyst and S Ligand. *J. Electrochem. Soc.* **1999**, *146*, 4473−4476.

(19) Love, J. C.; Estroff, L. A.; Kriebel, J. K.; Nuzzo, R. G.; Whitesides, G. M. Self-Assembled Monolayers of Thiolates on Metals as a Form of Nanotechnology. *Chem. Rev.* **2005**, *105*, 1103−1170.

(20) Morita, T.; Kimura, S. Long-Range Electron Transfer over 4 nm Governed by an Inelastic Hopping Mechanism in Self-Assembled Monolayers of Helical Peptides. *J. Am. Chem. Soc.* **2003**, *125*, 8732−8733.

(21) Nishizawa, M.; Sunagawa, T.; Yoneyama, H. Underpotential Deposition of Copper on Gold Electrodes through Self-Assembled Monolayers of Propanethiol. *Langmuir* **1997**, *13*, 5215−5217.

(22) Gu, Y.; Akhremitchev, B.; Walker, G. C.; Waldeck, D. H. Structural Characterization and Electron Tunneling at n-Si/SiO_2/SAM/Liquid Interface. *J. Phys. Chem. B* **1999**, *103*, 5220−5226.

(23) Janek, R. P.; Fawcett, W. R.; Ulman, A. Impedance Spectroscopy of Self-Assembled Monolayers on Au(111): Evidence for Complex Double-Layer Structure in Aqueous $NaClO_4$ at the Potential of Zero Charge. *J. Phys. Chem. B* **1997**, *101*, 8550−8558.

(24) Janek, R. P.; Fawcett, W. R.; Ulman, A. Impedance Spectroscopy of Self-Assembled Monolayers on Au(111): Sodium Ferrocyanide Charge Transfer at Modified Electrodes. *Langmuir* **1998**, *14*, 3011−3018.
(25) Góes, M. S.; Rahman, H.; Ryall, J.; Davis, J. J.; Bueno, P. R. A Dielectric Model of Self-Assembled Monolayer Interfaces by Capacitive Spectroscopy. *Langmuir* **2012**, *28*, 9689−9699.